Available online at www.sciencedirect.com

SciVerse ScienceDirect

Ceramics International 39 (2013) S239–S243

CERAMICS INTERNATIONAL

www.elsevier.com/locate/ceramint

Structural and magnetic properties of nanocrystalline zinc-doped metal ferrites (metal = Ni; Mn; Cu) prepared by sol–gel combustion method

Thanit Tangcharoen[a,*], Anucha Ruangphanit[b], Wisanu Pecharapa[a,c]

[a]*College of Nanotechnology, King Mongkut's Institute of Technology Ladkrabang (KMITL), Bangkok 10520, Thailand*
[b]*Thai Microelectronics Center (TMEC), Chachoengsao 24000, Thailand*
[c]*Thailand and Center of Excellence in Physics (ThEPCenter), CHE, 328 SiAyutthaya Road, Bangkok, Thailand*

Available online 16 October 2012

Abstract

In this work, nanocrystalline M–Zn ferrites (M = Ni; Mn; Cu) with compositions of $M_{1-x}Zn_xFe_2O_4$ ($x = 0.0$, 0.2 and 0.4) were synthesized from metal nitrate precursors by rapid the sol–gel combustion method using diethanolamine (DEA) as the fuel. As-synthesized powders were calcined at 1000 °C for 4 h. The crystal structures and morphologies of these compounds were characterized by X-ray diffraction (XRD) and field-emission scanning electron microscopy (FE-SEM), respectively. The chemical interaction of ferrite powders was investigated by Fourier transform infrared spectroscopy (FTIR). The magnetic properties of after-calcined nanoparticles were measured at room temperature using a vibrating sample magnetometer (VSM). The single phase spinel cubic structure formation is confirmed by XRD and FTIR results. Meanwhile FE-SEM micrographs show the appearance of both undoped and Zn-doped ferrite ceramic samples. In addition, the VSM analyses indicate that the Zn content has a significant influence on the magnetic properties such as saturation magnetization (M_s) and coercivity (H_c).

Keywords: A. Sol–gel processes; C. Magnetic properties; D. Ferrites

Introduction

Nickel, manganese and copper ferrites are kind of soft ferrimagnetic materials which have high resistivity, high dielectric constant, high initial permeability, high saturation magnetization and low power losses. This distinctive substance is vastly used in many applications such as electronic devices, computer devices, communication, space exploration and medication [1,2]. Generally, it is found that those metal ferrites have an inverse spinel cubic crystal structure in which half of the tetrahedral sites (A-sites) are occupied by half of Fe^{3+} ions. The octahedral sites (B-sites) will be held by the leftover Fe^{3+} with the transition metal ions (Ni^{2+}, Mn^{2+} or Cu^{2+}) [3]. In theory, the addition of appropriate transition metal ion into the spinel structure will generate the movement of many cations between two lattice sites and directly affect crucial properties especially magnetic behavior of ferrites [1].

Ferrites are usually synthesized by miscellaneous techniques such as co-precipitation process, hydrothermal synthesis and mechanical alloying. However, most of those techniques have complicated synthesis steps, use advanced instruments and take a long process time [2]. Synthesis of ferrite using urea, citric acid, glycine and tartaric acid as the fuel in combustion method was already reported [4,5]. However in terms of thermochemistry, diethanolamine (DEA) is one of the potential fuels because of its greater heat of combustion compared to other conventional fuels. The heat of combustion of diethanolamine is −6.00 kcal/g, whereas those of favoured fuels such as citric acid, urea or glycine are only −2.76, −2.98 and −3.24 kcal/g, respectively [4].

For this reason, Zn^{2+} ions were selected as the doping element for this work and our main goal is to synthesize the zinc-doped metal ferrites by the sol–gel combustion method using diethanolamine as the fuel with a basic apparatus and simple procedure that can reduce the synthesizes time and retain the spinel structure characteristics. Moreover, the influence of Zn^{2+} ions on the alteration of the structural

*Corresponding author. Tel.: +66 81 9030094; fax: +66 2 329 8265.
E-mail address: thanitt@hotmail.com (T. Tangcharoen).

0272-8842/$ - see front matter © 2012 Elsevier Ltd and Techna Group S.r.l. All rights reserved.
http://dx.doi.org/10.1016/j.ceramint.2012.10.069

and magnetic properties of as-prepared ferrites was investigated.

Experimental

The Zn-doped metal ferrites $M_{1-x}Zn_xFe_2O_4$(M = Ni; Mn; Cu) were prepared by the sol–gel combustion method using $Ni(NO_3)_2 \cdot 6H_2O$, $Mn(NO_3)_2 \cdot 4H_2O$, $CuN_2O_6 \cdot 3H_2O$, $Zn(NO_3)_2 \cdot 6H_2O$ and $Fe(NO_3)_3 \cdot 9H_2O$ as starting materials. For the synthesis of nanocrystalline ferrite, stoichiometric quantities of metal nitrate were dissolved in absolute ethanol (C_2H_5OH) to form 0.25 M precursor solution. Diethanolamine ($(HOCH_2CH_2)_2NH$, DEA) was added as a fuel into a solution. The molar ratio of metal nitrates to diethanolamine is 1:1. The mixed solution was constantly stirred at 200 °C using a magnetic stirrer to transform it into a dried gel and auto-combusted until dark-brown powders were obtained. As-synthesized powders were granulated using polyvinyl alcohol (PVA) as a binder and were pressed at a pressure of 3 t/cm^2 to form pellets. After that, those pellets were gradually heated to 550 °C for 1 h at the rate of 10 °C/min to remove the binder material. Finally, the temperature was raised to sintering temperature of 1000 °C and kept at this temperature for 4 h.

The phase formation of sintered ferrite pellets was investigated by X-ray diffraction (XRD). The chemical vibrational mode of ferrite samples was studied by Fourier transform infrared spectroscopy (FTIR). The morphology analysis was carried out by field-emission scanning electron microscopy (FE-SEM). Magnetic characterization was examined by a vibrating sample magnetometer (VSM).

Results and discussion

Fig. 1 shows XRD patterns for the ceramic ferrite samples of Zn-doped Ni, Mn and Cu ferrites. All of the samples show the characteristic reflections of spinel cubic crystal structure of ferrite. No strong diffraction peaks of other impurities are observed and the zinc substitution insignificantly affects the final crystal phase. The main spinel diffraction peaks appear at about 29.5°, 35.5°, 37.0°, 42.5°, 53.0°, 56.5°, 62.0°, 70.5°, 74.0° and 79.0°, which are attributed to the (220), (311), (222), (400), (422), (511), (440), (620), (533) and (444) planes, respectively and is in good accordance with other works [1,2]. The X-ray diffraction patterns show a slight shifting in peaks position due to unstable *d*-spacing values with increasing Zn content in all ferrite samples. Moreover, the crystallite size (*D*), interplanar distance (*d*) and lattice parameter (*a*) of all ferrite samples were calculated from the X-ray peak broadening of the (311) diffraction peak and are listed in Table 1.

From Table 1, it is observed that the average crystallite sizes estimated from XRD data for all ferrite samples are approximately 40–70 nm, which suggest that the products have nano-sized crystallite. When nickel ferrite was doped

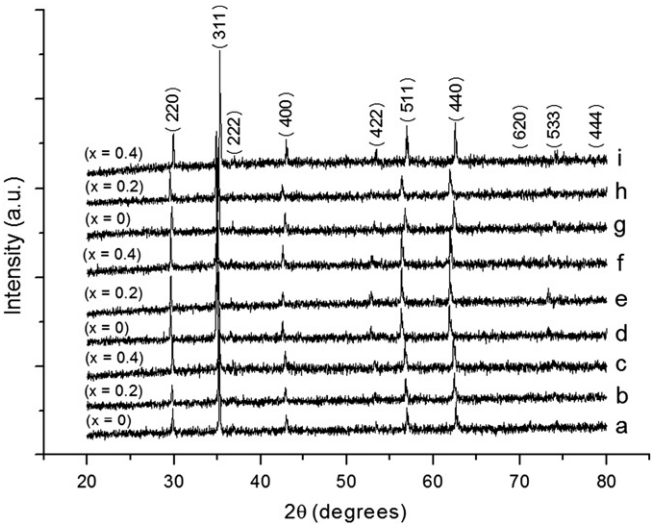

Fig. 1. XRD patterns of (a)–(c) $Ni_{1-x}Zn_xFe_2O_4$, (d)–(f) $Mn_{1-x}Zn_xFe_2O_4$ and (g)–(i) $Cu_{1-x}Zn_xFe_2O_4$ samples, where Zn concentration (*x*) is 0, 0.2 and 0.4.

by Zn^{2+} ions ($Ni_{1-x}Zn_xFe_2O_4$), the lattice parameter increases from 8.275 Å to 8.313 Å.

It is comprehensively considered that Zn^{2+} (0.82 Å) ion has larger ionic radius than does Ni^{2+} (0.78 Å) ion; the increase in Zn substitution content consequently results in lattice expansion [1]. This result is also consistent with the zinc-doped copper ferrite ($Cu_{1-x}Zn_xFe_2O_4$). When Cu^{2+} ions with ionic radius of 0.70 Å are replaced by the larger Zn^+ (0.82 Å) ions, the lattice parameter of this ferrite is significantly increased from 8.349 Å to 8.398 Å as listed in Table 1. However, it shows inconsistent results for the zinc-doped manganese ferrite ($Mn_{1-x}Zn_xFe_2O_4$). When Zn ions were added into the spinel crystal structure of this ferrite, the lattice parameter slightly decreased from 8.325 Å to 8.304 Å. This decrease may be attributable to the larger ionic radius of Mn^{2+} (0.91 Å) compared to Zn^{2+} (0.82 Å); thus the increase in Zn content can lead to noticeable lattice shrinkage in this ferrite [2].

In order to confirm the constitutions of spinel structure and to investigate the chemical properties of ferrite, the Fourier transform infrared (FTIR) spectroscopy of Zn-doped Ni, Mn and Cu ferrites was conducted in the wave number range of 400–800 cm^{-1} in transmittance mode and the corresponding results are shown in Fig. 2. In general, all zinc-doped metal ferrites samples exhibited three main characteristic absorption bands that confirm the existence of spinel structure. Firstly, the distinct band in 400 cm^{-1} range is assigned to the stretching vibration of Fe^{3+}–O^{2-} in the octahedral sites [5]. It is noticed that the intensity of this band increases when the Zn^{2+} ions are added into the spinel structure. This result may be explained by the fact that the increasing Zn^{2+} ions will replace some of the Fe^{3+} ions in tetrahedral sites and force them to octahedral sites which change and bear upon the absorption efficiency [6]. Secondly, the distinguishable band in 500–580 cm^{-1} is associated with the stretching vibration of

Table 1
Crystallite size (D), interplanar distance (d), lattice parameter (a), saturation magnetization (M_s) and coercive force (H_c) of zinc-doped metal ferrite samples.

Compound	x	D	d	a	M_s	H_c
		(nm)	(Å)	(Å)	(emu/g)	(Oe)
$Ni_{1-x}Zn_xFe_2O_4$	0	42.6	2.495	8.275	69.7	91.8
	0.2	42.2	2.500	8.292	100.3	48.2
	0.4	39.5	2.507	8.313	92.9	29.1
$Mn_{1-x}Zn_xFe_2O_4$	0	69.5	2.510	8.325	26.5	158.5
	0.2	53.9	2.508	8.317	104.2	47.6
	0.4	44.2	2.504	8.304	77.3	51.3
$Cu_{1-x}Zn_xFe_2O_4$	0	49.7	2.517	8.349	31.7	501.7
	0.2	39.8	2.524	8.373	60.4	36.3
	0.4	53.8	2.532	8.398	95.9	7.8

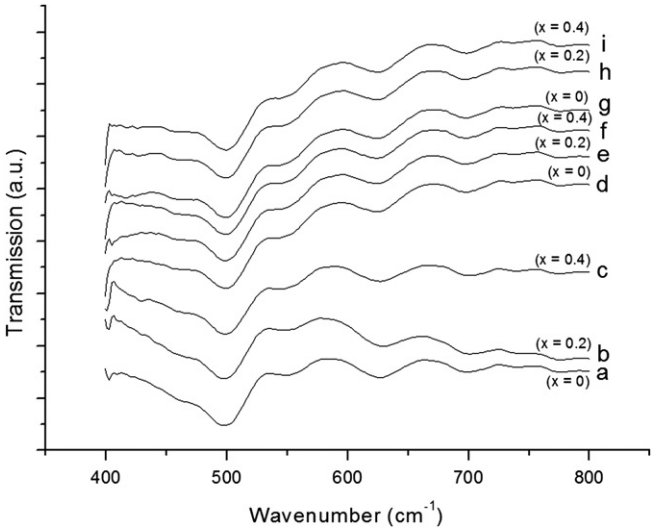

Fig. 2. FTIR spectra of (a)–(c) $Ni_{1-x}Zn_xFe_2O_4$, (d)–(f) $Mn_{1-x}Zn_xFe_2O_4$ and (g)–(i) $Cu_{1-x}Zn_xFe_2O_4$ samples where Zn concentration (x) is 0, 0.2 and 0.4.

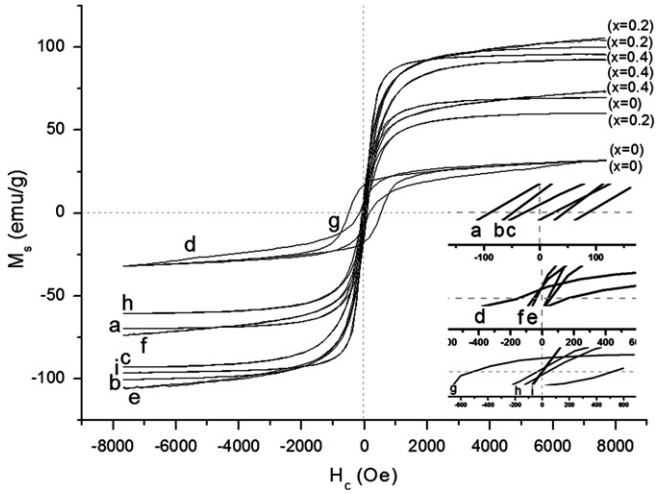

Fig. 3. Magnetization behavior of (a)–(c) $Ni_{1-x}Zn_xFe_2O_4$, (d)–(f) $Mn_{1-x}Zn_xFe_2O_4$ and (g)–(i) $Cu_{1-x}Zn_xFe_2O_4$ samples where Zn concentration (x) is 0, 0.2 and 0.4.

Fe^{3+}–O^{2-} in the tetrahedral sites [5]. The decrease in band strength with the increase of Zn^{2+} ions in the spinel structure is noticed. This feature may arise from the fact that some of the Fe^{3+} ions in the tetrahedral sites were substituted by Zn^{2+} ions and were driven to the octahedral sites, accompanying the considerable variation of absorption efficiency changing upon the decrease in Fe^{3+} ions [6]. There is another noticeable band at about 630 cm^{-1} which is ascribed to the stretching vibration of M^{2+}–O^{2-} (M = Ni, Mn or Cu) in the octahedral sites [7]. It is observed that this band was decreased when Zn^{+} ions increased because those transition metal ions were replaced by Fe^{3+} ions from the replacement by Zn^{2+} ions in the tetrahedral sites [6]. In addition, the existence of strange absorption bands at around 700–800 cm^{-1} is expected due to the vibrations of some contaminants which may originate from the incomplete reaction of combustion process.

Fig. 3 (a–i) illustrates the magnetic hysteresis loops of Zn-doped Ni, Mn and Cu ferrites. All of the magnetization curves show a normal S-shape type which is a ferrimagnetism characteristic. The saturation magnetization (M_s) and coercive force (H_c) results for each composition are listed in Table 1. From Table 1, it is seen that the maximum magnetization was obtained only with the incremental Zn^{2+} ions in spinel structure for all ferrite samples. The saturation magnetizations for Zn-doped Ni, Mn and Cu ferrites are 100.3, 104.2 and 95.9 emu/g which are found in $Ni_{0.8}Zn_{0.2}Fe_2O_4$, $Mn_{0.8}Zn_{0.2}Fe_2O_4$ and $Cu_{0.6}Zn_{0.4}Fe_2O_4$, respectively. This occurrence may be explained by the fact that when these metal ferrites are not doped by Zn^{2+} ions, half of the Fe^{3+} ions occupy all of tetrahedral sites (A-sites) and the remaining Fe^{3+} ions are held in half of the octahedral sites (B-sites) [3]. The net magnetic moments generated from 5 Bohr magnetons (μ_B) of Fe^{3+} ions will cancel each other and only the magnetic moment generated from Bohr magneton of any transition metal ions (Ni, Mn or Cu) which has rather low values will still remain[3]. However, when the metal ferrites are doped by Zn^{2+} ions, the additional Zn^{2+} ions can lead to the replacement of

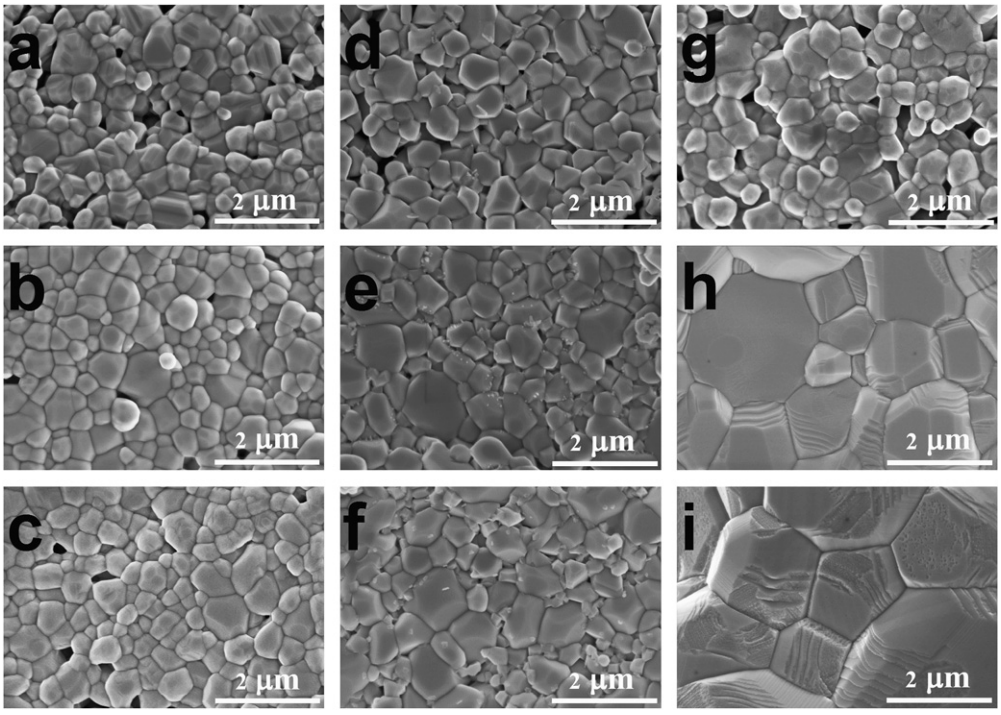

Fig. 4. FE-SEM photographs of (a)–(c) $Ni_{1-x}Zn_xFe_2O_4$, (d)–(f) $Mn_{1-x}Zn_xFe_2O_4$ and (g)–(i) $Cu_{1-x}Zn_xFe_2O_4$ samples where Zn concentration (x) is 0 (1st row), 0.2 (2nd row) and 0.4 (3rd row).

some Fe^{3+} ions in tetrahedral sites and push it to octahedral sites [5]. The difference of Fe^{3+} ions in both of lattice sites leads to the unequal magnetic moment at A and B sites and generates the net magnetic moment. The incorporation of additional magnetic moment with the original magnetization from the transition metal ions can lead to a drastic increase in the total magnetization for the zinc-doped metal ferrites with certain Zn composition [8]. In addition, the coercive forces for each ferrite samples are displayed as the insets in Fig. 3 and listed in Table 1. It is clearly seen that the coercive force tends to decrease with the increase of Zn ions. The minimum coercive forces for Zn-doped Ni, Mn and Cu ferrites are 29.1, 47.6 and 7.8 Oe which are found in $Ni_{0.6}Zn_{0.4}Fe_2O_4$, $Mn_{0.8}Zn_{0.2}Fe_2O_4$ and $Cu_{0.6}Zn_{0.4}Fe_2O_4$, respectively. It is presumably due to the alternation of particle and grain size of ferrite sample before and after the zinc doping. Compared to Ni, Mn and Cu ferrites (Fig. 4a, d and g), the larger particle size and grain size of Zn-doped Ni, Mn and Cu ferrites (Fig. 4c, e and i) could have more magnetic domains and domain walls, resulting easy demagnetization [7]. Fig. 4 shows FE-SEM photographs of Zn-doped Ni, Mn and Cu ferrites sintered ceramic samples with 20,000 times magnification. It is observed that the zinc increment affects morphologies of all ferrite samples especially the grain size. The microstructure of Zn-doped Ni and Mn ferrites (Fig. 4c and f) show the dense structure with good uniform grain size of 400 nm and few pores which slightly increase from the non-substitution. However, when zinc ions were added into the Cu ferrite, the grain size of CuZn ferrite great increased from 400 nm (Fig. 4g) to 2 μm (Fig. 4i) which resulted in the drastic decrease in the coercive force from 501.7 Oe to 7.8 Oe.

Conclusions

From this research, the sol–gel combustion method has been justified to be a simple and powerful procedure for synthesizing important zinc-doped metal ferrite samples from metal nitrates using DEA as the fuel with reduction of time consumption. All of the sintered ceramic ferrite samples show the formation of single-phase spinel cubic crystal structure with nano-sized crystallite. The substitutions of zinc ions in nickel, manganese and copper ferrites play important roles in the alternation and improvement of crystal structure, chemical interaction, morphologies and magnetic characteristic of these ferrites.

Acknowledgments

This work has partially been supported by Thai Microelectronics Center (TMEC) and National Nanotechnology Center (NANOTEC), NSTDA, Ministry of Science and Technology, Thailand, through its program of Center of Excellence Network and KMITL research fund. Authors would like to thank TMEC for FE-SEM measurement and Department of Physics, Kasetsart University (KU) for VSM measurement.

References

[1] M. Atif, M. Nadeem, R. Grössinger, R.S. Turtelli, Studies on the magnetic, magnetostrictive and electrical properties of sol–gel synthesized Zn doped nickel ferrite, Journal of Alloys and Compounds 509 (2011) 5720–5724.

[2] M.R. Syue, F.J. Wei, C.S. Chou, C.M. Fu, Magnetic, dielectric, and complex impedance properties of nanocrystalline Mn–Zn ferrites prepared by novel combustion method, Thin Solid Films 519 (2011) 8303–8306.

[3] Y. Li, J. Jiang, J. Zhao, X-ray diffraction and Mössbauer studies of phase transformation in manganese ferrite prepared by combustion synthesis method, Materials Chemistry and Physics 87 (2004) 91–95.

[4] C.C. Hwang, J.S. Tsai, T.H. Huang, Combustion synthesis of Ni–Zn ferrite by using glycine and metal nitrates—investigations of precursor homogeneity, product reproducibility, and reaction mechanism, Materials Chemistry and Physics 93 (2005) 330–336.

[5] T. Slatineanu, A.R. Iordan, M.N. Palamaru, O.F. Caltun, V. Gafton, L. Leontie, Synthesis and characterization of nanocrystalline Zn ferrites substituted with Ni, Materials Research Bulletin 46 (2011) 1455–1460.

[6] S.E. Shirsath, B.G Toksha, R.H Kadam, S.M Patange, D.R Mane, G.S Jangam, A Ghasemi, Doping effect of Mn^{2+} on the magnetic behavior in Ni–Zn ferrite nanoparticles prepared by sol–gel auto-combustion, The Journal of Physics and Chemistry of Solids 71 (2010) 1669–1675.

[7] P. Laokul, S. Maensiri, Aloe vera solution synthesis and magnetic properties of Ni–Cu–Zn ferrite nanopowders, Journal of Optoelectronics and Advanced Materials 11 (2009) 857–862.

[8] T. Jahanbin, M. Hashim, K.A. Matori, S.B. Waje, Influence of sintering temperature on the structural, magnetic and dielectric properties of $Ni0 \cdot 8Zn0 \cdot 2Fe_2O_4$ synthesized by co-precipitation route, Journal of Alloys and Compounds 503 (2010) 111–117.